Inorganic Chemistry

ARTICLE

pubs.acs.org/IC

EXAFS−XANES Evidence of in Situ Cesium Reduction in Cs−Ru/C Catalysts for Ammonia Synthesis

Ilenia Rossetti,*[,†,‡] Laura Sordelli,[‡] Paolo Ghigna,[§] Sonia Pin,[§] Marco Scavini,[†,‡] and Lucio Forni[†]

[†]Dipartimento Chimica Fisica ed Elettrochimica and INSTM Unit, Università degli Studi di Milano, via C. Golgi 19, I-20133 Milano, Italy

[‡]CNR-ISTM, via C. Golgi 19, I-20133 Milano, Italy

[§]Dipartimento Chimica and IENI-CNR, INSTM, Università degli Studi di Pavia, Vialle Taramelli 12, I-27100 Pavia, Italy

ABSTRACT: We present here a X-ray absorption spectroscopy (XAS) investigation on the local chemical order and electronic structure of Cs and Ba, promoters of the Ru/C catalysts for ammonia synthesis that attracted interest because of highly increased productivity. The role of the promoters is still largely unclear, although indirect evidence for Cs partial reduction has been obtained by this and other groups. Our XAS analysis with in situ H_2 reduction directly supports the partial Cs reduction in the promoted Ru/C catalysts, depending on the presence of Ru and on the graphitization degree of the support. Higher coordination of Ba was observed with respect to Cs in the reduced samples, without evidence of heavy atoms (Ru, Cs, and Ba) in the surroundings. Because of the strong electropositive nature of Cs, direct experimental evidence of its partial reduction is of outstanding significance also for other applications.

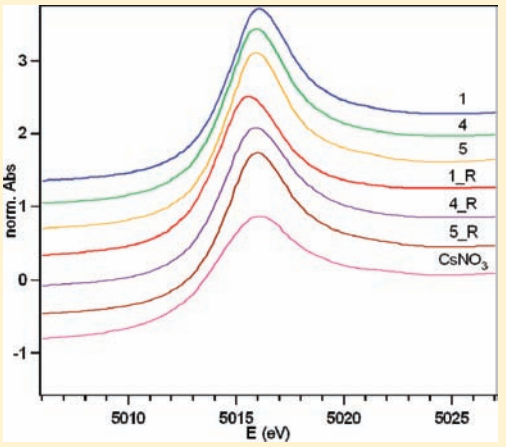

1. INTRODUCTION

Ammonia is traditionally produced by the Haber−Bosch process, a milestone of industrial chemistry,[1] based on N_2 reduction by H_2 mediated by an Fe-based catalyst. Supported Ru proved to be a valuable substitute for traditional catalysts, either leading to higher NH_3 productivity or allowing a decrease of the operating pressure, with a considerable decrease in production cost.[2−4] Good catalytic activity was obtained when Ru was supported on C, partially graphitized through a high-temperature treatment (at least 1900 °C) in order to improve its resistance toward methanation under the ammonia synthesis conditions (ca. 400−450 °C and 100−150 bar). Moreover, the addition of promoters is a must for obtaining a commercially acceptable conversion. In particular, the copresence of Cs and Ba has been suggested as a way for obtaining an optimal catalytic performance.[4,5]

It is currently accepted in the literature that the rate-determining step of the reaction is the dissociative adsorption of N_2, which is favored by the presence of the so-called B5 sites, located on the edges of Ru particles.[6] The dissociative adsorption of H_2 occurs on the same Ru particles, although in this case, no structure sensitivity is reported; i.e., no specific adsorption sites are evidenced. Because of the need for an excess negative charge on the active metal, required for the activation of N_2, transfer of the electron density from a promoter (electronic) to Ru seems beneficial.

On the basis of ab initio modeling and transmission electron microscopy analysis, it has been reported that Ba is likely localized as BaO on the Ru particles.[6] However, the actual role played by BaO, either "electronic"[6] or structural,[7], as well as its actual oxidation state, is still under debate. Indeed, recent reports advance the hypothesis that Ba may be found as a mixture of Ba^0 + BaO in activated, singly promoted Ba−Ru/C samples.[8] By contrast, it is usually supposed that Cs is located on the carbon support in the vicinity of Ru particles[4] as either cesium hydroxide, oxide, or more likely superoxide.

Following X-ray photoelectron microscopy (XPS) measurements, Cs is believed to be active as an electronic promoter because it donates a part of its electron density to Ru even in its oxidized form, at least according to some authors.[1,3,5,9] By contrast, other groups reported that, under the above-reported reaction conditions, Cs is fully or partially reduced, thus promoting more efficiently charge transfer to Ru.[4,7] Thermodynamic calculations[10,11] suggest that partial reduction of Cs could be mediated by H species coming from the dissociative chemisorption of H_2 on Ru. Reduced Cs atoms could then be stabilized by the formation of intercalation compounds in the graphitic layers.[7,12] Whatever is the charge-transfer mechanism, a possible reduction of Cs is hypothesized on the basis of the strong increase of H_2 uptake during the reduction step (temperature-programmed reduction, TPR) and O_2 uptake during the reoxidation step (O_2 chemisorption) for Cs-containing samples with respect to Cs-free ones.[7,12]

In summary, there is a hot debate in the literature on the location (local environment) and oxidation state of the promoters. This is

Received: January 24, 2011
Published: March 24, 2011

Table 1. Sample Composition and O_2 Uptake after Reduction at 400 °C

sample	support	Ru (wt %)	Cs (wt %)	Ba (wt %)	V_{O_2} ($N \cdot cm^3/g_{Ru}$)
1_Cs−Ru/GC	graphitized C	4.0	5.0		77.11
2_Ba−Ru/GC	graphitized C	4.0		4.0	61.76
3_Cs−Ba−Ru/GC	graphitized C	4.0	5.0	4.0	
4_Cs/GC	graphitized C		5.0		0.2*
5_Cs−Ru/AC	active C	4.0	5.0		52.42
6_Cs/AC	active C		5.0		0.2*
7_Ru/GC	graphitized C	4.0			41.83
8_Ru/AC	active C	4.0			51.18
9_GC	graphitized C				0.2*
10_AC	active C				0.2*

* Chemisorption data not referable to the Ru amount. Values are expressed as Ncm^3/g_{sample}.

due to the fact that all of the above-mentioned hypotheses have been mainly advanced on the basis of indirect evidence. Furthermore, because it is well-known that Cs is among the most electropositive elements of the periodic table, experimental evidence of its reduction should be considered of wide interest for the whole chemical community.

In situ X-ray absorption spectroscopy (XAS), considering both the extended X-ray absorption fine structure (EXAFS) and X-ray absorption near-edge structure (XANES) parts, can throw light on this point because of the possibility of investigating with atomic selectivity both the local chemical environment and the electronic structure. Therefore, powdered samples of various composition were investigated here by EXAFS−XANES spectroscopy at the Cs K- and L_3-edges and Ba K-edge. In order to check the effect of the graphitization degree of the support, i.e., the possible formation of intercalation compounds, Ru and Cs were supported on both an active C and a highly graphitized one. In addition, Ru free samples were analyzed as blank samples to check the possible mediation of chemisorbed H for Cs reduction.

2. EXPERIMENTAL SECTION

2.1. Catalyst Preparation. All of the samples were prepared by impregnation from aqueous solutions, using two different supports: a graphitized C, referred to as GC, with Brunauer−Emmett−Teller specific surface area (SSA) = 280 m^2/g and a commercial active C, referred to as AC, with SSA = 1400 m^2/g. Ru was deposited from an aqueous solution of $Ru(NO)(NO_3)_3$ (Aldrich; diluted HNO_3 solution) as described in detail elsewhere,[13] achieving a final Ru/C loading of ca. 4 wt %. The sample was reduced in flowing H_2 at 320 °C for 5 h. The Ru/GC sample was split into different portions, which were impregnated with only one single promoter (Cs or Ba) from an aqueous solution of the corresponding nitrate ($CsNO_3$, Sigma, purity >99.5%; $Ba(NO_3)_2$, Aldrich, purity >99%). Another portion was impregnated with both promoters, and a final one was left unpromoted. The promoters/Ru atomic ratios, optimized in a previous work,[5] were Cs/Ru = 1 and Ba/Ru = 0.6 (mol/mol). Cs-promoted blank samples, i.e., without Ru, were also prepared with both supports (Table 1).

2.2. Catalyst Characterization. The samples were characterized by TPR and O_2 chemisorption, following the procedure detailed in refs 12 and 14. Briefly, TPR was carried out by means of a homemade apparatus on ca. 0.15 g of catalyst (0.15−0.25 mm particle size), in 40 cm^3/min of a 5% H_2/Ar gas mixture, by heating (10 °C/min) up to 400 °C for 1 h (Ar, SAPIO, purity ≥99.9995 vol %; H_2, SAPIO, purity ≥99.9995 vol %). Sample reduction was followed by flushing in He (SAPIO, purity ≥99.9999 vol %), and the samples were then cooled to 0 °C for pulsed O_2 chemisorption (SAPIO, purity ≥99.999 vol %). The outcoming gas during both TPR and chemisorption analysis was monitored and quantified by means of a thermal conductivity detector (TCD).

Activity tests were carried out as described in ref 5 on a bench-scale, continuous, fixed-bed downflow Incoloy 800 reactor. The catalyst, ground and sieved into 0.15−0.25 mm particles, was loaded into the reactor after dilution (1/22, v/v) with quartz powder of the same particle size. The catalyst was activated by flowing H_2/N_2 (1.5/1, v/v), at gas hourly space velocity (GHSV) = 20 000 h^{-1} and 30 bar, while the temperature was increased by 1 °C/min up to 450 °C, kept for 5 h, and then decreased to 430 °C (N_2, SAPIO, purity ≥99.9995 vol %). Activity tests were carried out under standard reaction conditions, i.e., 100 bar and 430 °C, by varying the gas mixture space velocity from GHSV = 30 000 to 200 000 h^{-1}. The effluent gas was analyzed by absorption in a known amount of diluted H_2SO_4, followed by titration of the residual acid with NaOH.

2.3. XAS Experiments. *2.3.1. K-Edges.* XAS spectra at the Cs and Ba K-edges were recorded at Beamline BM29 of the European Synchrotron Radiation Facility (ESRF, Grenoble, France). A quartz tubular reactor (1 cm i.d. and 20 cm length) was filled with ca. 1 g of fresh sample and continuously fed with 30 mL/min of a 10 vol % H_2/He mixture. A first EXAFS spectrum was collected on the fresh sample at room temperature. The temperature was then raised by 10 °C/min up to either 400 or 450 °C and kept for 1 h. XANES spectra were collected every 30 °C or 15 min during the heating and isothermal steps. After cooling at room temperature, an EXAFS spectrum was recorded after reduction. The data collection was made in transmission mode using a Si(511) double-crystal monochromator, 10% detuned for harmonic rejection, with ion chambers as detectors, with a constant step in k in the EXAFS range, and collecting at least two spectra for each sample in every condition. A gas cell filled with Xe was used for energy calibration at the Xe K-edge.

2.3.2. Cs L_3-Edge. XAS spectra at the Cs L_3-edge were collected at the XAFS beamline of the ELETTRA synchrotron facility in Trieste (Italy) with a Si(311) double-crystal monochromator and ion chamber detectors. Third-harmonic rejection was achieved by 30% detuning. A Ti metal foil was permanently used during the spectra acquisition for the angle/energy calibration and to take into account a possible difference in the thermal loading of the monocromator. The Ti foil was measured simultaneously with all of the samples with a postreference ionization chamber detector, and each spectrum was calibrated with respect to the energy position of the Ti edge (which was always found constant within 0.01 eV). All spectra were recorded at room temperature in transmission mode at the Cs L_3-edge over the range 4.85−6.35 keV (so including also the L_2- and L_1-edge regions), with an energy sampling step of 0.15 eV at the edge and an integration time of 2−3 s per point. Three spectra per sample were acquired.

dx.doi.org/10.1021/ic2001656 |Inorg. Chem. 2011, 50, 3757–3765

The samples were analyzed both as-prepared (preactivated at 400 °C in 40 mL/min of 5 vol % H_2/Ar and stored under an inert atmosphere) and further reduced in situ with a heating rate of 7.5 °C/min up to 400 °C, kept for 1 h, in 60 mL/min of the 5 vol % H_2/Ar mixture, and cooled under the same gas mixture.

In situ sample reduction was carried out inside a reaction cell designed for XAS measurements, under controlled conditions as similar as possible to those of the gas−solid catalytic reaction in a plug-flow fixed-bed reactor (a gas-flow system for gas throughput longitudinal to the sample-holder axis, a mass flow controller system for remote gas selection/mixing, and a remote Eurotherm-controlled heating−cooling system).

Samples, in fine powder form, were loaded into a 1-mm-long sample holder, inserted into the reaction cell equipped with Be windows and a graphite septum, thus providing an optimal total absorption of 2.5.

2.3.3. Data Analysis. The raw spectra were obtained by point-to-point connection with straight lines, without any smoothing. For XANES analysis at the Cs K- and L_3-edges, the spectra were first preedge subtracted, by fitting the preedge background with a straight line, and then normalized to give a unit absorption jump at the edge position. The energy edge position was determined as the first inflection point. For EXAFS data analysis, at all of the investigated edges, EXAFS was extracted using the *ATHENA* code.[15] Data analysis was made using the *EXCURVE* program.[16] Phases and amplitudes were calculated by the program making use of the muffin-tin model, in the framework of the Hedin−Lundquist and Von Bart aproximations for the exchange and ground-state potentials, respectively.[15] This includes the effects of inelastic losses due to electron inelastic scattering (photoelectron mean-free path). The fittings were made in the k space, using a k^2 weighting scheme. The stability of the fits was checked by testing different weighting schemes and verifying that the fitting parameters were recovered within errors. The $S_0{}^2$ parameter was always found to be the unit within error. The accuracy of the phase shifts and amplitudes was tested by fitting the $CsNO_3$ Cs L_3- and K-edge EXAFS spectra and recovering the crystallographic distances within 0.01 Å.

Considering the Δk and Δr intervals of each fit, the number of EXAFS independent points can be estimated as always to be larger than 6, while the number of independent fitting parameters was lower than or equal to 6 in every fit. The goodness of fit (GOF) was estimated by the *EXCURVE* Rk^2 parameter, which was found to be on the order of the unit for each fit.

3. RESULTS AND DISCUSSION

During a preliminary investigation of the role of promoters in Ru/C catalysts for ammonia synthesis, we evidenced the need for electronic promotion to achieve an optimal ammonia yield. Indeed, the addition of Ba (0.6 mol/mol with respect to Ru) brought about an increase of the ammonia concentration in the outlet gas from 1.8 vol % (unpromoted sample) to 10.5 vol %, at 430 °C and 100 bar, H_2/N_2 = 1.5 vol/vol, and GHSV = 30 000 h^{-1}. The further addition of Cs (1.0 mol/mol) improved conversion up to 11.7 vol %.[5]

XPS data collected on activated samples evidenced a red shift of the Ru binding energy when all of these promoters were added separately, but the highest effect (−0.3 eV) was observed with Cs, even in its oxidized form.[5]

Later, when setting up an O_2 chemisorption procedure for determination of Ru dispersion, we observed some O_2 overuptake for the promoted samples, with respect to the unpromoted ones.[14] Furthermore, a different reduction pattern was observed during TPR analysis of some Cs-promoted samples. Indeed, the decomposition temperature of the Cs precursor and H_2 uptake was found to be fully dependent on the catalyst formulation. Similar results were independently obtained by other authors.[9,17] Therefore, we started an extensive investigation of the effect of catalyst reduction on the oxidation state of the promoters. The main findings are reported below.

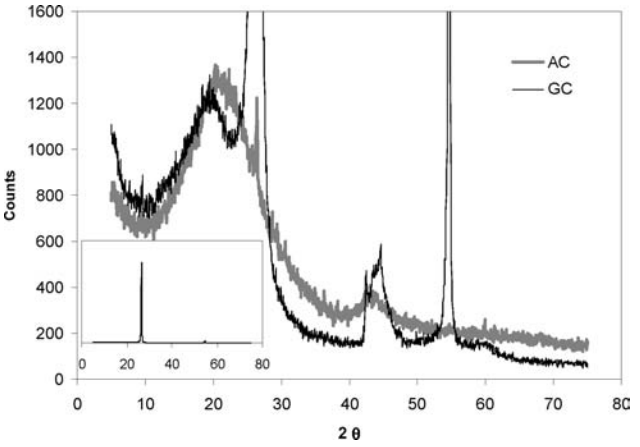

Figure 1. XRD patterns of the AC and GC supports. Inset: full-scale pattern of the GC sample.

The X-ray diffraction (XRD) patterns of both supports are also reported in Figure 1, in order to qualitatively define the graphitization degree. The AC sample was almost completely amorphous, whereas typical reflections of graphite appeared for the GC sample, with an intensity of 1.4 × 10^5 of the main peak (see the inset in Figure 1), indicating a high graphitization degree.

3.1. TPR and O_2 Chemisorption. The as-prepared samples were activated during a TPR run up to 400 °C. The analysis evidenced, when relevant, the decomposition of the nitrate precursors and the reduction of ruthenium oxides. The bare C supports did not show any H_2 uptake in the investigated temperature range. The quantification of H_2 consumption cannot be easily ascribed to the different reduction contributions because the decrease of the H_2 concentration due to reduction is not distinguishable from NO_x emission due to nitrate decomposition. However, the patterns can be interpreted at least qualitatively. A much higher H_2 uptake has been observed for the Cs-promoted sample 1_Cs−Ru/GC with respect to sample 4_Cs/GC during catalyst reduction at 400 °C (Figure 2a). The comparison between samples 5_Cs−Ru/AC and 6_Cs/AC showed relatively similar results but with a much lower intensity (Figure 2b, notice the different scale). Precursor decomposition also occurred at lower temperature, when Ru was present, with respect to Cs/C samples, as was already pointed out elsewhere.[7] The reduction of RuO_x was evident at low temperature only for unpromoted samples, with this contribution overlapping with a much broader signal in the case of Cs-promoted catalysts.

O_2 chemisorption experiments (Table 1) evidenced a much higher O_2 uptake for sample 1_Cs−Ru/GC with respect to sample 7_Ru/GC. O_2 uptakes by samples 5_Cs−Ru/AC and 8_Ru/AC were substantially similar. The blank samples constituted by the bare supports before and after Cs addition showed much smaller O_2 consumption.

Such results have been interpreted on the basis of partial reduction of Cs(I) during the preliminary TPR, followed by its reoxidation during O_2 chemisorption experiments. In spite of the intriguing statement and the support of independent results,[9,12,17] a final proof of this model had not yet been proposed until now. The following XAS measurements were then carried out to validate these findings.

dx.doi.org/10.1021/ic2001656 |*Inorg. Chem.* 2011, 50, 3757–3765

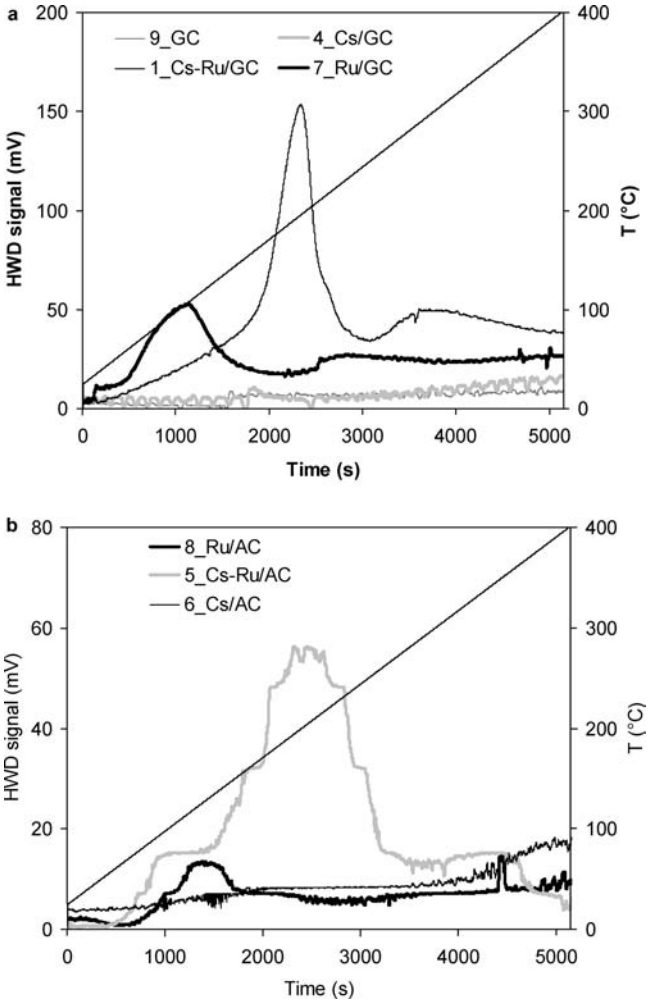

Figure 2. TPR−TCD patterns of selected samples.

3.2. XAS Analysis. XANES spectra at the Cs K-edge for sample 1_Cs−Ru/GC are shown in Figure 3a, reported for selected temperatures during in situ reduction. The room temperature spectra of the same catalyst as such and after the thermal cycle are also reported in Figure 3b, where the inset shows the corresponding derivatives. Unfortunately, it is readily noted that the reduction procedure induces smearing of the spectral features. In addition, as a result of the core−hole broadening at the Cs K-edge, which is very large, even more than 14 eV, the Cs K-edge is almost featureless. This also holds for the Ba K-edge spectra (Figure 4), meaning that any possible energy shift of the edge caused by variation in the Cs or Ba oxidation state would be entirely masked by the core−hole broadening. This behavior is found also for all of the other samples, with minor differences from sample to sample, with the differences being a little bit more evident for the Cs K-edge. This result has the direct meaning that the local chemical environments of Cs and Ba are rather similar in different samples. However, the major effect of the core−hole broadening makes analysis of the EXAFS part of the spectra very difficult, in particular for the reduced samples.

As a consequence, a different strategy has been attempted, by concentrating our attention to the Cs L_3-edge, showing a much smaller core−hole broadening (ca. 2.7 eV). However, in situ

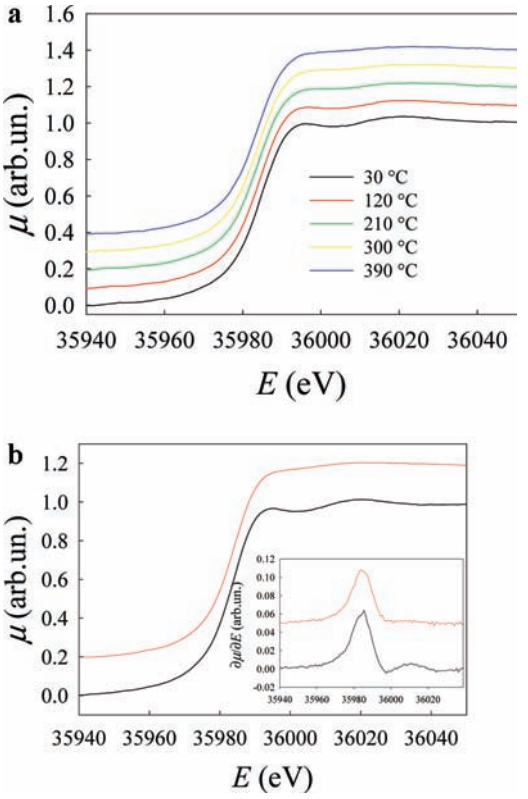

Figure 3. (a) Cs K-edge XANES spectra of sample 1_Cs−Ru/GC collected at different temperatures during in situ reduction. (b) XANES spectra at the Cs K-edge for sample 1_Cs−Ru/GC, as such (bottom line) and after the thermal treatment described in the Experimental Section (upper line). The inset shows the corresponding derivatives.

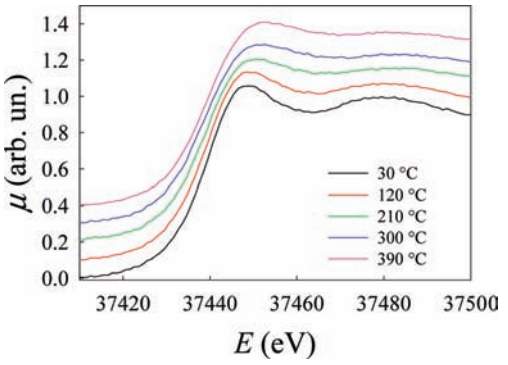

Figure 4. Ba K-edge XANES spectra of sample 2_Ba−Ru/GC collected at different temperatures during in situ reduction.

analysis in such a low energy range (close to 5 keV) required the careful design of an environmental chamber, transparent in this energy region, but with sufficient retainment of gas flow. This goal was accomplished at the ELETTRA syncrotron facility in Trieste, Italy.

Some explorative tests were first made by collecting the spectra on preactivated samples, holding them in a quartz microreactor under a H_2 atmosphere, and then transferring them into an analytical cell in a glovebox under an inert gas. No difference was observed in the XAS spectra with respect to the as-prepared catalysts.

dx.doi.org/10.1021/ic2001656 |*Inorg. Chem.* 2011, 50, 3757–3765

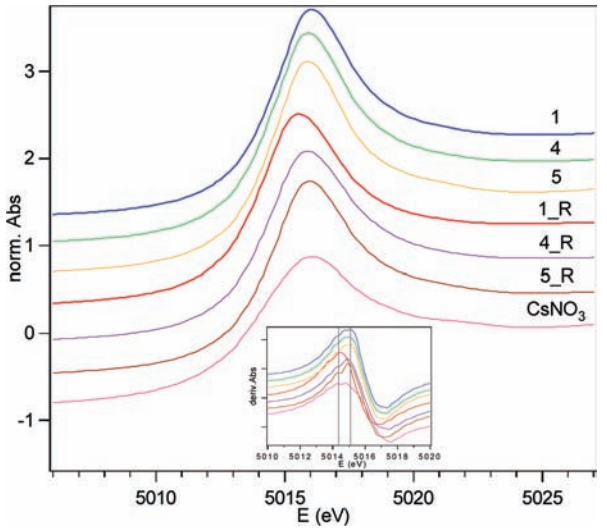

Figure 5. XANES spectra at Cs L_3-edge of samples 1_Cs−Ru/GC, 4_Cs/GC, and 5_Cs−Ru/AC, collected before and after (postscript "R") in situ reduction. The inset shows the corresponding derivatives.

Therefore, an in situ reduction treatment was performed by collecting the spectra under the continuous flow of a reducing gas mixture. Sample activation was carried out as described in the Experimental Section, and cooling to room temperature was then done under the same atmosphere.

The Cs L_3-edge XANES spectra are reported in Figure 5. Looking at the inset (derivative curves), one may notice that $CsNO_3$ gives rise to a rather symmetric absorption edge. By contrast, the nonreduced samples 1_Cs−Ru/GC, 4_Cs/GC, and 5_Cs−Ru/AC show a relatively sharp feature at ca. 5015 eV (right vertical line) accompanied by a tail toward lower energy. After reduction, the latter contribution is much less evident, leaving the edge shape much more sharp for every sample. In the case of the reduced sample 1_Cs−Ru/GC, one may further notice that the edge shape is identical with those of samples 4_Cs/GC and 5_Cs−Ru/AC after reduction but rigidly shifted to lower energy.

Indeed, identical Cs absorption edge energy values were observed before and after in situ catalyst activation for the Ru-free samples, even when the support was constituted by graphitized C (Figure 5, samples 4_Cs/GC and 4_Cs/GC_R), although a decreasing intensity of the white line was observed, attributed to a decrease of the d state density involved in the 2p−3d resonance transition. Identical behavior and comments hold also for the Ru-containing catalyst, supported on active C (Figure 5, samples 5_Cs−Ru/AC and 5_Cs−Ru/AC_R). By contrast, a net shift by ca. 0.5 eV of the absorption edge toward lower energy was observed for sample 1_Cs−Ru/GC after in situ reduction and a similar decrease of the white line intensity was observed. Such a shift is significant because at these energies the monochromator position reproducibility is 0.01 eV and the collection step is 0.15 eV, corresponding to the intrinsic monochromator resolution. Furthermore, the possible edge shift due to instrumental reasons was ruled out by simultaneously acquiring a reference spectrum (Xe for the K-edge experiments and a Ti foil for the L_3-edge spectra).

To better quantify the shift of the edge position, XANES spectra have been fitted with a combination of a Lorentzian curve for the line shape of the preedge resonance and an arc-tangent

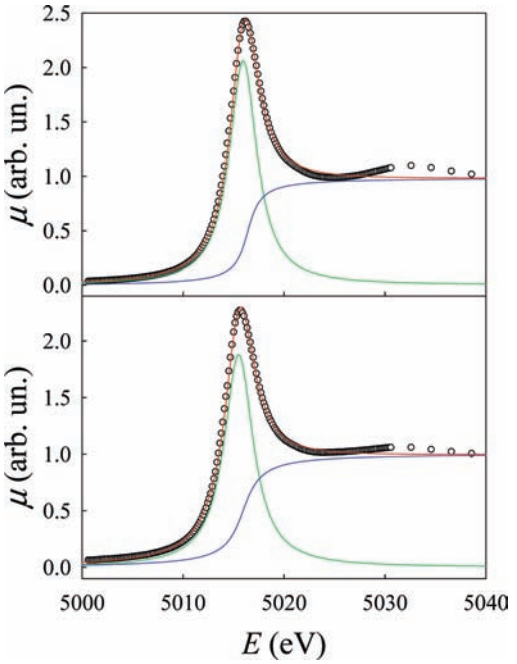

Figure 6. Fits of the XANES spectra at the Cs L_3-edge as described in the text: (upper panel) sample 1_Cs−Ru/GC as such; (lower panel) same sample but after in situ reduction. Hollow circles are the experimental points, the red curves the total fits, and the green and blue curves the Lorentzian and arc-tangent functions for the spectral shape of the white line and the absorption edge, respectively.

curve for the edge.[18−20] Figure 6 shows this fitting for sample 1_Cs−Ru/GC before (upper panel) and after the reduction (lower panel). The hollow circles are the experimental points, the red curves the total fittings and the green and blue curves the Lorentzian and arc-tangent curves, respectively. The edge positions, as measured by the inflection points of the arc-tangent curves are 5016.4 and 5015.9 eV before and after the reduction, respectively, thus confirming the 0.5 eV shift toward lower energies mentioned above.

This behavior is consistent with the Cs(I) presence in every as-prepared sample (see the $CsNO_3$ spectrum in Figure 5 as a reference material). After reduction, no variation of the Cs oxidation state can be inferred in the absence of Ru or when the sample was supported on activated C.

By contrast, we can deduce at least partial Cs reduction for the Cs-promoted Ru/GC sample after in situ reduction (catalyst 1_Cs−Ru/GC). Indeed, the energy position of an absorption edge in the XAS spectrum is affected by the well-known "chemical shift", the edge shifting to lower energy as the oxidation state decreases, reflecting the variations in the screening of the core electron−nucleus Coulombic interaction by the valence electrons. Therefore, the results here proposed can be seen as direct evidence of Cs partial reduction upon catalyst activation. This occurs in the presence of Ru, likely because of activation of H_2 by dissociative chemisorption and spillover in the presence of graphitic layers, stabilizing the reduced Cs for a time lapse sufficient for its detection.

The role of Ru is witnessed also by the above-summarized TPR tests, which showed that the decomposition temperature of the promoter precursor $CsNO_3$ occurred at much lower temperature in the presence of Ru than for Cs/C samples.[7,12] The

dx.doi.org/10.1021/ic2001656 |*Inorg. Chem.* 2011, 50, 3757–3765

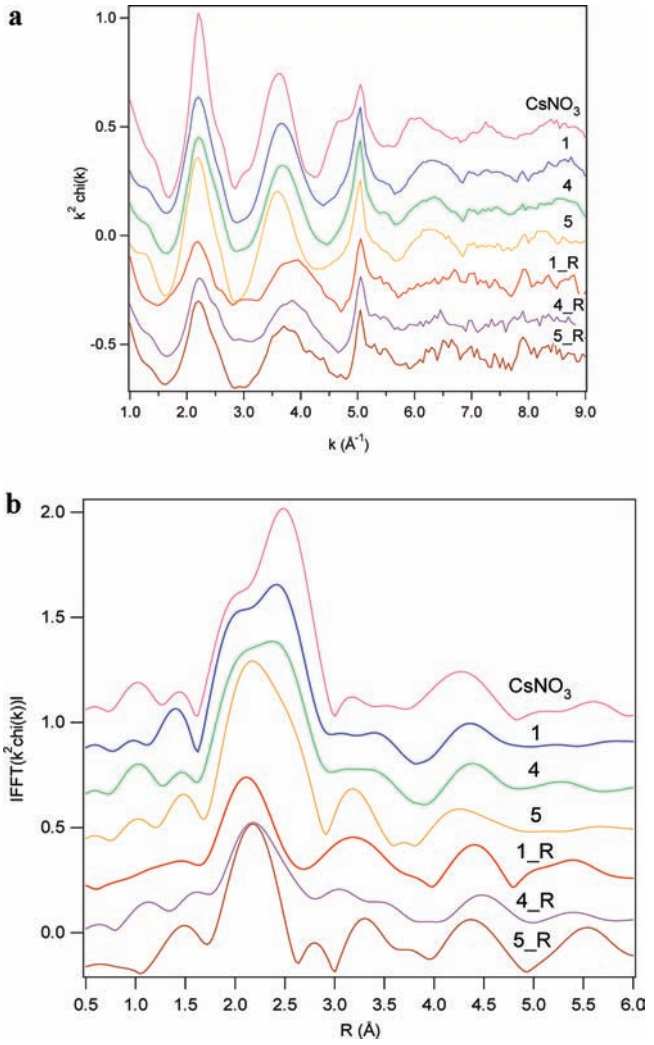

Figure 7. (a) EXAFS spectra at the Cs L_3-edge of samples 1_Cs−Ru/GC, 4_Cs/GC, and 5_Cs−Ru/AC, before and after (postscript "R") in situ reduction. (b) FFT of the Cs L_3-edge EXAFS spectra of samples 1_Cs−Ru/GC, 4_Cs/GC, and 5_Cs−Ru/AC, before and after (postscript "R") in situ reduction. Not phase-corrected.

latter effect can be explained by the formation of a possible $M^+\cdots C^-$ charge-transfer complex, in which partial reduction of the promoter salt is supported by the high heat of formation of the carbon−alkali complex.[1]

EXAFS data analysis was performed by fitting both the K- and L_3-edge spectra, for the as-prepared samples. For the Cs L_3-edge, the signal was elaborated up to the value of $k = 9.3$ Å^{-1} due to the near-L_2-edge. The spectra at the K-edge showed detectable oscillations up to $k \cong 10$ Å^{-1}. The spectra and their Fourier transform (FT) are reported in Figure 7.

The low intensity of the EXAFS spectra is in line with the presence of a few light atoms around Cs in the reduced sample 1_Cs−Ru/GC. Furthermore, the good quality of the spectra at the L_3-edge (signal-to-noise ratio ca. 10^4) evidences the presence of multiple excitation effects in the extracted EXAFS signal.[21]

The fittings were carried out by considering the contributions of the first neighbors up to 4 Å. It worth describing in some detail the fitting procedure that was used. The main problem here is determination of the coordination numbers from EXAFS analysis, which is not trivial, especially when the limited k range available is taken into account. Indeed, the coordination numbers in EXAFS are poorly determined because they are affected by several correlations as fitting parameters, for example, by the Debye−Waller (DW) factors, but also by the edge jump.[22] Therefore, a quite complex procedure for EXAFS analysis was used, aiming at avoiding the aforementioned correlations. In particular, the coordination numbers were fixed to certain values, and then EXAFS was fitted. This procedure was repeated for different values of the coordination numbers until the best agreement was obtained, as determined by the GOF parameter. As such, the errors in the coordination numbers were estimated to be ±1. In addition, attempts made to fit simultaneously the coordination numbers and the DW factors unavoidably resulted in unphysical values (for example, negative DW factors).

Whenever possible, both EXAFS at both of the edges were fit simultaneously with the same model. This is one of the advantages given by the *EXCURVE* code that we used for the fits. The results in Table 2 for the as-prepared samples refer to these multiple-edge fits. For the reduced samples, the simultaneous fit of the Cs K- and L_3-edge EXAFS spectra was not possible because of the reduced amplitude of the EXAFS oscillations, which, combined with broadening due to the core−hole lifetime, prevented us from reasonably extracting EXAFS at the Cs K-edge.

The fit quality is shown in Figure 8, as an example of the several fits done using different k ranges and different k weights. The results were always identical within error for all of the fits, even after increasing the k range. Several EXAFS fittings were made by previous removal of this multiple excitation according to refs 19 and 23−25. The results of these fits agree within experimental

Table 2. EXAFS Fitting Results[a]

edge	ΔE_0 (eV)	bond	N	distance (Å)	$2\sigma^2$ (Å^2)
		Sample 1_Cs−Ru/GC			
Cs K	7(2)*	Cs−C	2	2.91(2)	0.006(6)
Cs L_{III}	4(1)**				
Cs K	*	Cs−C	2	3.11(2)	0.004(6)
Cs L_{III}	**				
		Sample 1_Cs−Ru/GC after in Situ Reduction			
Cs L_{III}	9(3)*	Cs−C	2	2.82(6)	0.032(8)
	*	Cs−C	2	3.45(5)	0.06(4)
		Sample 4_Cs/GC			
Cs K	5(2)*	Cs−C	2	2.91(3)	0.011(5)
Cs L_{III}	3(1)**				
Cs K	*	Cs−C	2	3.12(3)	0.005(4)
		Sample 4_Cs/GC after in Situ Reduction			
Cs L_{III}	9(3)*	Cs−C	2	2.76(4)	0.040(7)
	*	Cs−C	2	3.43(4)	0.025(9)
		Sample 5_Cs−Ru/AC			
Cs K	9(2)*	Cs−C	2	2.89(2)	0.008(3)
Cs L_{III}	4(1)**				
Cs K	*	Cs−C	2	3.09(2)	0.004(3)
		Sample 5_Cs−Ru/AC after in situ reduction			
Cs L_{III}	7(2)	Cs−C	2	2.87(3)	0.017(5)

[a] C and O were almost equivalent in the model. Errors are given in parentheses. Stars indicate that the same value holds for different coordination shells.

dx.doi.org/10.1021/ic2001656 |*Inorg. Chem.* 2011, 50, 3757–3765

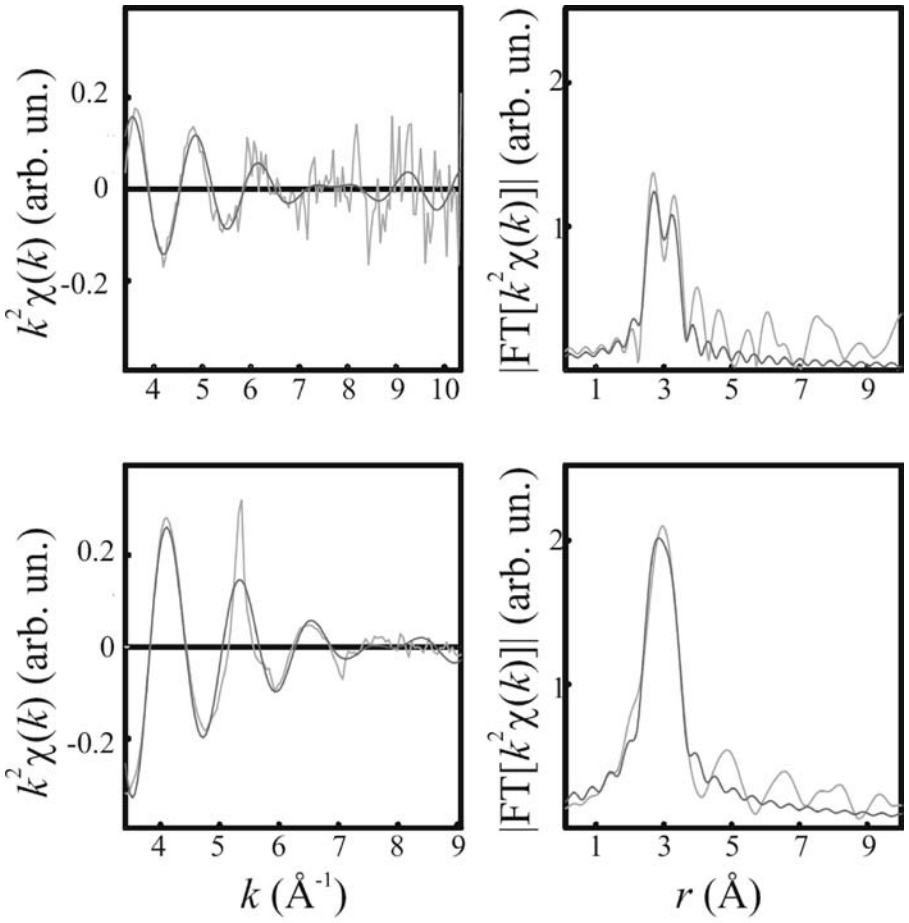

Figure 8. EXAFS fitting for sample 1_Cs−Ru/GC. Light-gray line: experimental fit. Dark-gray line: fit according to the model of Table 2. Both of the fits at the Cs K-edge (up) and Cs L_3-edge (bottom) are shown. Left: EXAFS spectra. Right: corresponding FT.

error with those of Table 2. All of the as-prepared samples showed about two C (or O) atoms located at about 2.9 Å and two C (O) atoms at 3.1 Å from the photoabsorber (Table 2). Unfortunately, it is not possible to distinguish the scattering contribution of C atoms from that of O atoms. The main effect after reduction is a net increase of the disorder, as is apparent in looking at the decreasing amplitudes of the EXAFS FT in Figure 7b. Coupled to the large core−hole broadening at the K-edge, this increase of the disorder inhibited effective EXAFS extraction for the Cs K-edge spectra of the reduced samples, as mentioned above. The effect of the disorder was pretty similar for the reduced samples 1_Cs−Ru/GC and 4_Cs/GC (see Table 2). In addition, for these two samples, the reduction caused a decrease of ca. 0.1 Å in the radial distance for the first Cs−C shell and an increase of ca. 0.4 Å for the second Cs−C shell. For sample 5_Cs−Ru/AC, we observed a concomitant decrease in coordination upon reduction and a smaller increase in disorder. In this case, the spectrum could be fitted with just one C (O) atom shell at ca. 2.9 Å. The above findings account for the different shapes of the EXAFS FT of Figure 7b.

This behavior supports the XANES evidence of reduction of part of Cs, as well as the formation of a suboxide, as suggested elsewhere.[7,26,27] In both cases, the effect would be an enhanced electron transfer to Ru, which would impart higher activity by decreasing both the activation barrier for N_2 adsorption and the stability of the adsorbed NH_x intermediates, with their prompt desorption freeing a higher amount of active sites and thus increasing the turnover frequency in ammonia synthesis.

It is also interesting to observe that the presence of heavy neighbors around Cs can be excluded. By contrast, the EXAFS spectra are compatible with Cs incorporation into the support, at least in part. This can additionally favor the charge transfer to Ru, provided the proper electron conductivity is available, such as for deeply graphitized C. As a matter of fact, the presence of metallic Cs cannot be claimed also because of the lack of vicinal Cs−Cs interaction but rather a partial reduction that can be accounted for with the changes in the local chemical environment of Cs that are observed in EXAFS. To rule out the possible effect of the particle size, possibly influencing the "end state" of the sample, all of the catalysts have been treated in the same way. If the particle size was changed as a result of sintering, the same effect should have been observed for each of them. Furthermore, the comparison between the local environment and its variation upon in situ reduction is provided by elaboration of the EXAFS data. Though a decrease in the local order may be concluded in every case after reduction, the XANES shift of the edge is evident only in some cases, for which a reduction cause has been invoked (compare, e.g., samples 1_Cs−Ru/GC and 4_Cs/GC in Table 2).

The local chemical environment of Ba, as inferred by EXAFS analysis of the Ba K-edge, shows a quite different situation. Indeed, the coordination number of Ba was much larger than that of Cs. In this case, 9−10 light atoms could be detected in the first

dx.doi.org/10.1021/ic2001656 |*Inorg. Chem.* 2011, 50, 3757–3765

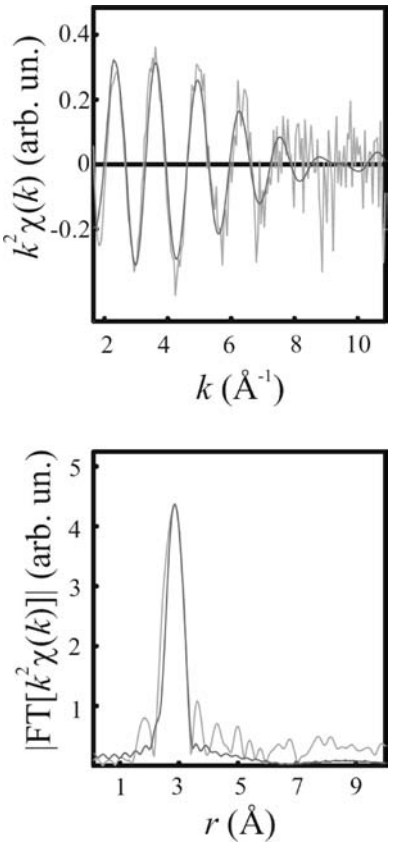

Figure 9. Ba K-edge EXAFS fitting for sample 2_Ba-Ru/GC. Light-gray line: experimental fit. Dark-gray line: fit according to the model of Table 3.

Table 3. Ba EXAFS Fitting Results

edge	ΔE_0 (eV)	bond	N	distance (Å)	$2\sigma^2$ (Å^2)
		Sample 2_Ba−Ru/GC			
Ba K	−4(3)*	Ba−C	4	2.85(2)	0.004(6)
	*	Ba−C	6	3.02(2)	0.007(6)
		Sample 2_Ba−Ru/GC after in Situ Reduction			
Ba K	−9(1)*	Ba−C	2	2.40(3)	0.009(6)
	*	Ba−C	7	2.65(3)	0.031(4)
		Sample 3_Cs−Ba−Ru/GC			
Ba K	−0.4(3)*	Ba−C	4	2.81(1)	0.004(1)
	*	Ba−C	6	2.97(1)	0.007(5)
		Sample 3_Cs−Ba−Ru/GC after in Situ Reduction			
Ba K	−0.4(3)*	Ba−C	4	2.74(1)	0.011(3)
	*	Ba−C	6	2.91(1)	0.020(4)

coordination shell. Figure 9 shows an example of the Ba K-edge EXAFS spectrum and its Fourier transform (sample 2_Ba−Ru/GC, as prepared). The fit, according to the parameters summarized in Table 3, is also shown. Also, in this case, no evidence of heavy atoms in the neighboring Ba could be observed.

The two Ba-containing samples here considered (samples 2_Ba−Ru/GC and 3_Cs−Ba−Ru/GC, before and after Cs addition, respectively) were different for their behavior upon reduction. Indeed, on the one hand, a large variation in the local chemical environment was found in sample 2_Ba−Ru/GC (without Cs). In this instance, a marked decrease in the distance between Ba and its first neighbors was detected, along with a substantial increase of the local disorder. This was somewhat analogous to what happened to Cs in the Cs-containing samples. On the other hand, for sample 3_Cs−Ba−Ru/GC, containing both promoters, the reduction induced a much less pronounced variation of the local chemical environment of Ba, with the coordination distances remaining almost unchanged and the increase of disorder being much smaller.

Such data evidence that when Ba is the only promoter, it may act as an electronic promoter, a role entrusted mainly to Cs in the doubly promoted samples, where the electronic modifications of Ba seem less important. This seems to be in agreement with the possible BaO reduction suggested for singly promoted Ba−Ru/C samples, which was not observed in the case of multiply doped samples.[4,8]

XAS analysis provides an averaged picture of the Cs and Ba states. However, the model we propose here is based on promoter reduction mediated by H species (as suggested in the literature). The latter form by chemisorption on Ru and then migrate to the support by spillover. This picture limits the amount of Cs ions, which may be reduced to those relatively near to Ru. This is even more important because the electron density gained upon partial reduction may be given back to Ru in order to enhance its ability to coordinate N.

We should also notice that these catalysts normally operate at very high hydrogen pressure, typically in excess of 50 bar. Therefore, under the usual working conditions, the $P_{H_2}/P_{oxygenates}$ partial pressure ratio is very high. O_2 may indeed be present either in molecular form or, more likely, as water, a good oxidizing agent for alkaline metals. This partial pressure ratio is 2−3 orders of magnitude higher in a real catalytic reactor than it would be in a typical laboratory-scale TPR apparatus or in an EXAFS in situ cell of the type described here. The extent of Cs or Ba reduction may be very sensitive to this partial pressure ratio, so it is possible that the extent of reduction of the working catalyst cannot be achieved in the characterization equipment adopted here. Nevertheless, when concluding that promoter partial reduction can take place, we adopt a conservative approach, with the extent of reduction under the real operating conditions being possibly even higher although not quantifiable.

As a final remark, we may stress that XANES at the Cs L_3-edge has direct access to the empty s and d density of states projected onto Cs. The edge shift observed is thus indicative of an increased electron density on Cs upon reduction. This is direct evidence of partial reduction of Cs, which was inferred as an indirect result by our and other groups.[28] The above evidence is quite equivalent to the claim that Cs acts as a promoter via an electronic mechanism, rather than acting on the structure of the catalyst. We, however, have to warn that the amount of such a reduction is difficult if not impossible to evaluate. In fact, on the one hand, calculation of the XANES manifold would require detailed knowledge of the medium-range structure around Cs, information that is clearly impossible to retrieve. On the other hand, a comparison with standard compounds would require measurement of XANES on well-characterized Cs−C compounds in different chemical environments, which is made impossible by the lack of sufficient details in the literature.

Indeed, known and stable Cs^+ compounds are systems by far different from that under study. This is exemplified by the absorption edge of $CsNO_3$, which correctly indicates the edge position, correlated to the oxidation state, but is useless to assess the local structure. CsO_x compounds are not stable and show

dx.doi.org/10.1021/ic2001656 |Inorg. Chem. 2011, 50, 3757–3765

a poorly defined stoichiometry, so they are not suitable as standards.

A further complication comes from the spatial confinement of the intercalated Cs. Indeed, every attempt to structurally characterize Cs-containing compounds would represent the three-dimensional arrangement of the material, by far different from the conformation of intercalated ions or atoms. Similar arguments are extensively discussed in ref 29. Furthermore, even if three-dimensional clusters could form between graphite layers, they would likely be very distorted.

Some examples of Cs−graphite intercalation compounds have been recently reviewed,[30] although a definite assessment of their structure is not yet provided, mainly because their arrangement is predominantly bound to the statistics of diffusion within the host matrix. Therefore, the only representative materials that could be used as reference (Cs−graphite intercalation compounds) are not usable as well-defined standards. In addition, they are not stable and are difficult synthesize as pure materials.

Nevertheless, an ever-growing interest toward Cs doping of C structures (e.g., nanotubes) is demonstrated by the number of recent publications on modification of the electronic properties of such doped materials,[31−34] which reinforces the impact of the present findings also in very different application fields.

4. CONCLUSIONS

A set of Ru-based catalysts active for ammonia synthesis have been characterized by different techniques. Cs-promoted catalysts supported on graphitized C showed oversized H_2 uptake during reduction and larger O_2 uptake during chemisorption. This behavior was limited or not observed when supporting the catalyst on active C or in the absence of Ru.

XAS analysis at both Cs K- and L_3-edges was carried out under in situ reduction conditions similar to those used during TPR and for catalyst activation. This allowed one to soundly support the hypothesis of Cs partial reduction under the ammonia synthesis operating conditions, until now advanced only by indirect measurements.

Depending on the catalyst formulation, a strong reduction of Cs coordination was observed after reduction, together with an increase of the local disorder. A rather similar effect was observed with the Ba-promoted sample, but to a much lower extent for the (Cs + Ba)-promoted sample.

Therefore, both of these promoters may exert an electronic effect on Ru under the ammonia synthesis reaction conditions, by partial reduction and further donation of the electronic density to the active metal. When the support is highly graphitized, a reduced Cs intermediate may be stabilized by the formation of intercalation compounds, allowing its direct identification.

AUTHOR INFORMATION

Corresponding Author

*E-mail: ilenia.rossetti@unimi.it. Fax: +39-02-50314300.

ACKNOWLEDGMENT

The ELETTRA synchrotron light laboratory in Basovizza (Trieste, Italy) and the ESRF facility in Grenoble (France) are gratefully acknowledged for providing the beamtime, along with the staff of the XAFS and BM29 beamlines for their technical assistance.

REFERENCES

(1) Tennison, S. R. In *Catalytic Ammonia Synthesis, Fundamentals and Practice*; Jennings, J. R., Ed.; Plenum Press: New York, 1991; p 303.
(2) Rossetti, I.; Pernicone, N.; Ferrero, F.; Forni, L. *Ind. Eng. Chem. Res.* **2006**, *45*, 4150.
(3) Aika, K.; Shimazaki, K.; Hattori, Y.; Ohya, A.; Ohshima, S.; Shirota, K.; Ozaki, A. *J. Catal.* **1985**, *92*, 296.
(4) Kowalczyk, Z.; Krukowski, M.; Raróg-Pilecka, W.; Szmigiel, D.; Zielinski, J. *Appl. Catal., A* **2003**, *248*, 67.
(5) Rossetti, I.; Pernicone, N.; Forni, L. *Appl. Catal., A* **2001**, *208*, 271.
(6) Hansen, T. W.; Hansen, P. L.; Dahl, S.; Jacobsen, C. J. H. *Catal. Lett.* **2002**, *84*, 7.
(7) Raróg-Pilecka, W.; Mskiewicz, E.; Jodzis, S.; Petryka, J.; Łomot, D.; Kaszkur, Z.; Karpínski, Z.; Kowalczyk, Z. *J. Catal.* **2006**, *239*, 313.
(8) Truszkiewicz, E.; Raróg-Pilecka, W.; Schmidt-Szalowski, K.; Jodzis, S.; Wilczkowska, E.; Lomot, D.; Kaszkur, Z.; Karpinski, Z.; Kowalczyk, Z. *J. Catal.* **2009**, *265*, 181.
(9) Guraya, M.; Sprenger, S.; Raróg-Pilecka, W.; Szmigiel, D.; Kowalczyk, Z.; Muhler, M. *Appl. Surf. Sci.* **2004**, *238*, 77.
(10) Shitova, N. B.; Bobrynkin, N. M.; Noskov, A. S.; Prosvirin, T. P.; Bukhtiyarov, V. I.; Kochubel, D. T.; Tsyrulínikov, P. G.; Shlyapin, D. A. *Kinet. Catal.* **2004**, *45*, 414.
(11) Hikita, T.; Kadowaki, Y.; Aika, K. *J. Phys. Chem.* **1991**, *95*, 9396.
(12) Rossetti, I.; Mangiarini, F.; Forni, L. *Appl. Catal., A* **2007**, *323*, 219.
(13) Rossetti, I.; Forni, L. *Appl. Catal., A* **2005**, 315.
(14) Rossetti, I.; Pernicone, N.; Forni, L. *Appl. Catal., A* **2003**, *248*, 97.
(15) http://cars9.uchicago.edu/~ravel/software/exafs/.
(16) Binsted, N.; Hasnain, S. S. *J. Synchrotron Radiat.* **1996**, *3*, 185.
(17) Lomot, D.; Karpinski, Z.; Raróg-Pilecka, W.; Szmigiel, D.; Kowalczyk, Z. *Pol. J. Chem.* **2004**, *78*, 163.
(18) Pantelouris, A.; Kiiper, G.; Hormes, J.; Feldmann, C.; Jansen, M. *J. Am. Chem. Soc.* **1995**, *117*, 11749.
(19) Kodre, A.; Padežnik Gomilšek, J.; Arčon, I.; Aquilanti, G. *Phys. Rev. A* **2010**, *82*, 022513.
(20) Ghigna, P.; Spinolo, G.; Scavini, M.; Tamburini, U. A.; Chadwick., A. V. *Physica C* **1995**, *253*, 147.
(21) Padežnik Gomilšek, J.; Arčon, I.; Kodre, A. *Acta Chim. Slov.* **2006**, *53*, 18.
(22) Ghigna, P.; Di Muri, M.; Spinolo, G. *J. Appl. Crystallogr.* **2001**, *34*, 325.
(23) Padežnik Gomilšek, J.; Kodre, A.; Bukovec, N.; Kozjek Škofic, I. *Acta Chim. Slov.* **2004**, *51*, 23.
(24) Arčon, I.; Kodre, A.; Padežnik Gomilšek, J.; Hribar, M.; Mihelič, A. *Phys. Scr.* **2005**, *T115*, 235.
(25) Solera, J. A.; García, J.; Proietti, M. G. *Phys. Rev. B* **1995**, *51*, 2678.
(26) Larichev, Yu. V.; Shlyapin, D. A.; Tsyrul'nikov, P. G.; Bukhtiyarov, V. I. *Catal. Lett.* **2008**, *120*, 204.
(27) Larichev, Yu. V.; Prosvirin, I. P.; Shlyapin, D. A.; Shitova, N. B.; Tsyrul'nikov, P. G.; Bukhtiyarov, V. I. *Kinet. Catal.* **2005**, *46*, 597.
(28) Szmigiel, D.; Bielawa, H.; Kurtz, M.; Hinrichsen, O.; Muhler, M.; Raròg, W.; Jodzis, S.; Kowalczyk, Z.; Znak, L.; Zielinski, J. *J. Catal.* **2002**, *205*, 205.
(29) Bichoutskaia, E.; Pyper, N. C. *J. Chem. Phys.* **2008**, *129*, 154701.
(30) Sangster, J. *J. Phase Equilib. Diffus.* **2008**, *29*, 93.
(31) Sato, Y.; Suenaga, K.; Bandow, S.; Iijima, S. *Small* **2008**, *4*, 1080.
(32) Khazaei, M.; Farajian, A. A.; Kawazoe, Y. *Phys. Rev. Lett.* **2005**, *95*, 177602.
(33) Kim, S. H.; Choi, W. I.; Kim, G.; Song, Y. J.; Jeong, G.-H.; Hatakeyama, R.; Ihm, J.; Kuk, Y. *Phys. Rev. Lett.* **2007**, *99*, 256407.
(34) Ih Choi, W.; Ihm, J.; Kim, G. *Appl. Phys. Lett.* **2008**, *92*, 193110.